THE JOURNAL OF PROSTHETIC DENTISTRY

RESEARCH AND EDUCATION

Misfit simulation on implant-supported prostheses with different combinations of engaging and nonengaging titanium bases: Part 3: A radiographic evaluation

Vygandas Rutkunas, DDS, PhD,[a] Daniel Kules, DDS,[b] Ingrida Mischitz, DDS,[c] Sandra Huber, DMD, MS,[d] Marta Revilla-León, DDS, MSD, PhD,[e] Christel Larsson, DDS, PhD,[f] and Martin Janda, DDS, PhD[g]

ABSTRACT

Statement of problem. The fit of implant-supported prostheses plays an important role in their mechanical and biological stability. Clinically, the prosthetic fit is typically assessed radiographically, but this method relies on the operator's subjective evaluation. Whether available digital tools could optimize the evaluation of the prosthetic fit is uncertain.

Purpose. The purpose of this in vitro study was to evaluate the influence of an image processing program on the radiographic detection of discrepancies in the active and passive fit of implant-supported prostheses. Two-implant-supported screw-retained prostheses were analyzed by simulating the vertical and horizontal misfits of 3 different implant abutment configurations.

Material and methods. Seven casts were fabricated using 2 internal-connection titanium implants: 1 control; 3 with vertical (V) misfit of 50 μm, 100 μm, 150 μm; and 3 with horizontal (H) misfit of 35 μm, 70 μm, 100 μm. Thirty bar-shaped zirconia frameworks were fabricated and divided into 3 groups (n=10) according to their attachment to 2 engaging (E-E), 2 nonengaging (NE-NE), and engaging and nonengaging (E-NE) titanium bases. Digital parallel periapical radiographs were made of each specimen in the passive and active fit situation on each cast (1-screw test), except for the E-E specimens, which were only seated on the control, H35, and H70 casts because the fit on the remaining casts was poor. The mean gray value (MGV) was measured at the chosen regions of interest on the second implant (side B) using the ImageJ software program. Differences in the MGV measurements between the passive and active conditions were tested using a *t* test (α=.05) and compared the different misfit levels using analysis of variance (1-way ANOVA), followed by the Tukey HSD test (α=.05).

Results. The highest values for the differences between passive and active fit were found for the V150 and H100 misfit simulations ($P<.05$). Statistical differences between the MGVs were found with some exceptions: the smallest simulated misfits (H35 and V50) revealed statistically significant MGV differences from the highest simulated misfits (V150, H100) and from the H70 in the groups where an engaging component was present ($P>.05$). In the horizontal misfit group of NE-NE abutment configuration, H70 revealed no significant difference from the control group cast ($P>.05$).

Conclusions. Measuring MGV differences between passive and active fit could be a promising alternative for detecting 70- to 150-μm gaps in the implant-abutment connection that result from the misfit. However, the procedure was not adequate for detecting < 50 μm gaps, cannot be uniformly applied to all types of implant-abutment connections, and requires 2 exposures to X-radiation. (J Prosthet Dent 2025;133:222-228)

We, the authors of this manuscript, declare that we have no conflicts of interest that could inappropriately influence or bias the results, discussion, or interpretation of this research. This work has been conducted in an unbiased and transparent manner, without any financial, personal, or professional interests that could be perceived as having a potential influence on the research outcomes or the content of this manuscript. We affirm that we have received no financial or in-kind support from any organization that could have a direct or indirect interest in the research reported in this paper. Additionally, we have not held any affiliations, memberships, or any other associations with groups or organizations that might pose a conflict of interest.

Supported by the Lithuanian Buisiness Support Agency, grant Nr. J05-LVPA-K-01-0055 and the DIGITORUM research, grant Nr. MTTP SK.

[a]Professor, Department of Prosthodontics, Institute of Odontology, Faculty of Medicine, Vilnius University, Vilnius, Lithuania; and Director, Digitorum Research Center, Vilnius, Lithuania.

[b]Postgraduate student, Department of Periodontology, Faculty of Medicine, Vilnius University, Vilnius, Lithuania; and Researcher, Digitorum Research Center, Vilnius, Lithuania.

[c]Dental Research Assistant, Department of Dental Medicine and Oral Health, Medical University of Graz, Graz, Austria.

[d]Attending, Department of Dental Medicine and Oral Health, Medical University of Graz, Graz, Austria.

[e]Affiliate Professor, Graduate Prosthodontics, Department of Restorative Dentistry, School of Dentistry, University of Washington, Seattle, Wash.; Faculty and Director, Digital Dentistry, Kois Center, Seattle, Wash.; and Affiliate Professor, Graduate Prosthodontics, Department of Prosthodontics, School of Dental Medicine, Tufts University, Boston, Mass.

[f]Associate Professor, Faculty of Odontology, Malmö University, Malmö, Sweden; and Associate Visiting Professor, Faculty of Dentistry, Department of Prosthetic Dentistry, Riga Stradins University, Riga, Latvia.

[g]Assistant Professor, Faculty of Odontology, Malmö University, Malmö, Sweden.

Clinical Implications

A method of measuring the difference in MGVs between active and passive fit can detect misfits that are currently considered of clinical significance. As potential misfits can be masked by tightening the prosthesis, radiographic examination of a passive fit with only 1 screw tightened is important. MGV measurements along with artificial intelligence tools can aid in the clinical detection of misfits.

The main goal of implant prosthodontics is the long-term success of implant-supported restorations. However, error propagation during the clinical and laboratory steps of implant-supported prosthesis fabrication inevitably results in misfits at the implant-abutment interface (IAI),[1–4] leading to microgaps between the implant and abutment and increased strains and stresses in the components of the prosthesis.[1,5–9] Microgaps may open because of loading forces, leading to micromovements at the IAI.[10] Furthermore, misfits have been reported to lead to mechanical complications such as screw loosening or fractures[11–13] or biological complications such as peri-implant tissue inflammation associated with microleakage and the accumulation of periodontal pathogens.[14–17] Zirconia is becoming an increasingly popular restorative material for implant-supported fixed dental prostheses (FDPs),[18] a material likely to be particularly sensitive to the stresses and strains caused by an ill-fitting framework because of its brittle nature.[19]

Screw-retained implant-supported FDPs use combinations of engaging (E) and nonengaging (NE) abutments. Using various E and NE abutment combinations in 2-implant-supported FDPs has been reported to be associated with prosthetic fit and biomechanics, with using E abutments in both implants having the best stress distribution in finite element analysis[20]; however, using E abutments in both implants is the most affected by horizontal and vertical misfit,[21] hindering or even preventing the insertion of such a prosthesis. Using NE abutments in both implants has been reported to result in the smallest microgaps and screw rotation angles, making it the best performing combination in misfit situations.[21,22] However, the NE-NE combination is the least mechanically stable[23,24] it has been reported to exhibit the highest stresses in implant-prosthesis components.[20] Because of the antirotational properties of the E abutment, E-NE combinations have shown better stability than NE-NE combinations, which could reduce the risk of screw fractures.[20,23–25]

Commonly used in vitro methods for misfit detection include stereomicroscopy,[21] optical microscopy,[26] scanning electron microscopy,[27] dental radiography,[28–32] X-ray microtomography,[1,7,33] and the screw-resistance test.[22] In clinical settings, a combination of techniques may be used to assess the fit of implant prostheses, including visual inspection, the use of an explorer, alternate finger pressure, the 1-screw test, the screw-resistance test, and dental radiography.[34,35] Radiographic misfit detection may vary depending on the clinician performing the test and the angulation of the X-ray beam relative to the implant components.[28,29,36] Microgaps of 13 μm can be detected if the angulation is no more than 5 degrees,[28] whereas a gap of 20 μm at the IAI of an internal connection implant at an angle of 15 degrees has been reported to be undetectable.[29] Therefore, keeping the beam perpendicular to the implant axis as much as possible is important for accurate microgap detection.[32,36] Notably, the fit of the implant-level restorations on implants with internal connections is much more difficult to assess as the connection is located subgingivally.

The use of image processing software programs should be developed to improve the diagnosis of misfit with digital dental radiology. Promising results have been achieved by applying artificial intelligence using periapical images in implant system identification,[37–39] evaluating peri-implant bone loss around implants,[10] and identifying fractured implants.[40] However, the authors are unaware of studies on using image processing programs in dental radiology for the quantitative evaluation of implant prosthesis misfit.

The purpose of the study was to assess the microgap at the IAI of a 2-implant-supported 3-unit zirconia prosthesis with different combinations of E and NE abutments and different levels of simulated horizontal and vertical misfits in active and passive fit situations using an image processing program. Mean gray value (MGV) measurements were used to evaluate the microgaps in the regions of interest (ROI) in dental radiographic images. The null hypothesis was that MGV measurements would not show significant differences between the passive and active fit conditions with different misfit levels for the E-NE, E-E, and NE-NE combinations of abutments.

MATERIAL AND METHODS

The material and methods of the present study were based on those used in a previous study.[21] A total of 30 2-implant-supported bar-shaped zirconia (KATANA Zirconia HT; Kuraray Noritake Dental Inc) specimens were cemented on Ø4.3×2-mm titanium bases (Conelog; CAMLOG Biotechnologies GmbH and divided into 3 groups (n=10) according to different abutment combinations: E-E, E-NE, and NE-NE. For each specimen, the implant bases were marked as side A (on the

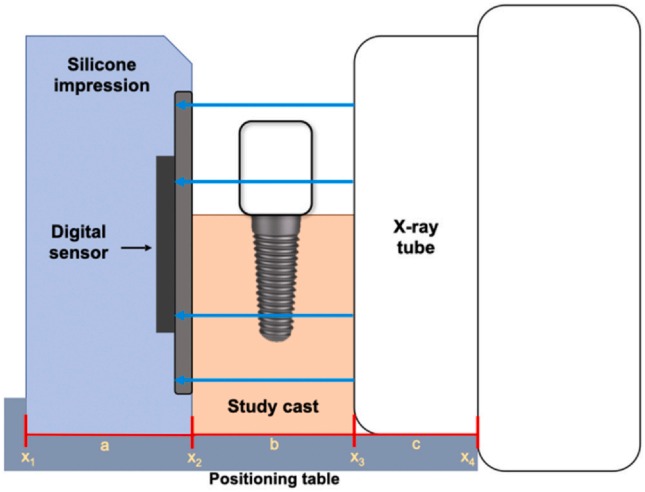

Figure 1. Sagittal view of positioning table with x_1, x_2, x_3, and x_4 specific locations of digital sensor, study cast, and X-ray tube. Distance a=35 mm, distance b=30 mm, and distance c=200 mm.

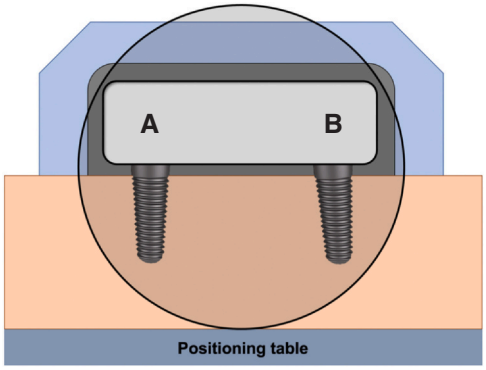

Figure 2. Frontal view of positioning table. *Black circle* represents position of X-ray tube. Implant on side B angled 10 degrees toward implant on side A.

left) and side B (on the right) (Fig. 1). In the E-NE group, the E base was on side A, and the NE base was on side B.

The fit of each specimen was tested on the control group (no misfit) and on 6 definitive casts simulating 50-, 100-, and 150-µm vertical (V) and 35-, 70-, 100-µm horizontal (H) misfit levels. The E-E specimens were excluded from the H100, V50, V100, and V150 simulated misfit groups, as the nonpassive fit was obvious in these scenarios.

A digital dental X-ray machine (ProX; Planmeca Oy) was used to assess the passive and active fit of the FDPs on different casts radiographically. The images were obtained at 63 kV, 6 mA, and an exposure time of 0.4 second. The digital sensor (Planmeca ProSensor, Size 1; Planmeca Oy) was attached to silicone impression material (Variotime Easy Putty; Kulzer GmbH). A special positioning table was constructed to ensure the same position for the digital sensor, the cast, and the dental X-ray tube (Figs. 1, 2). Two radiographs were made for each model: passive fit - the abutment screw on side A was tightened to 10 Ncm while the abutment located on side B was left without a screw; and active fit - both abutment screws were tightened to 20 Ncm (the final torque value recommended by the manufacturer). New screws were used for each specimen. The passive and active fit were evaluated by measurements of the MGVs of 8-bit X-ray at 2 specific areas in the implant-abutment connection (left and right) on implant B using a specific software program (ImageJ version 1.53e; National Institutes of Health). The mean values of these 2 locations were used in further statistical analysis. The MGV indicates the brightness of a selected image area; it is the sum of the gray values of all the pixels in the selection divided by the number of pixels. Gray values range from 0 (absolute black) to 255 (absolute white) pixels.

All measurements of passive and active fit were made on side B of the implant bilaterally; however, the specific measurement locations were different because of the different designs of the E and NE abutments (Fig. 3). In the groups with the E abutment on the B side, the area of measurement was in the implant-abutment connection area, while in the groups with the NE abutments on the B side, the area of measurement was slightly occlusal to the conical connection. The area measured on the E abutments was unsuitable for NE abutments because of the short internal part of the NE abutment and the free internal space, which could have distorted the data. Equal areas (144 square pixels) were used for MGV measurements at the NE and E abutment sites.

The normal distribution of MGVs was tested by using the Shapiro-Wilk test, and the equality of variances was assessed with the Levene test. The differences (unsigned mean values) in MGVs between the passive and active fit of the same group were used for the statistical analysis. The differences between the passive and active fit groups were tested by a paired samples *t* test. These values were compared between the different misfit levels separately for each abutment combination (E-E, E-NE, and NE-NE) using analysis of variance 1-way ANOVA, followed by the Tukey HSD test. All statistical analyses were performed using a statistical software program (IBM SPSS Statistics for Windows, v27; IBM Corp) (α=.05).

RESULTS

Mean values of MGV differences between the passive fit and active fit situations in the groups are presented in Figure 4 and Table 1. For the vertical passive to active misfit, no significant differences between the V50 group and the control groups and between the V50 and V100 values were

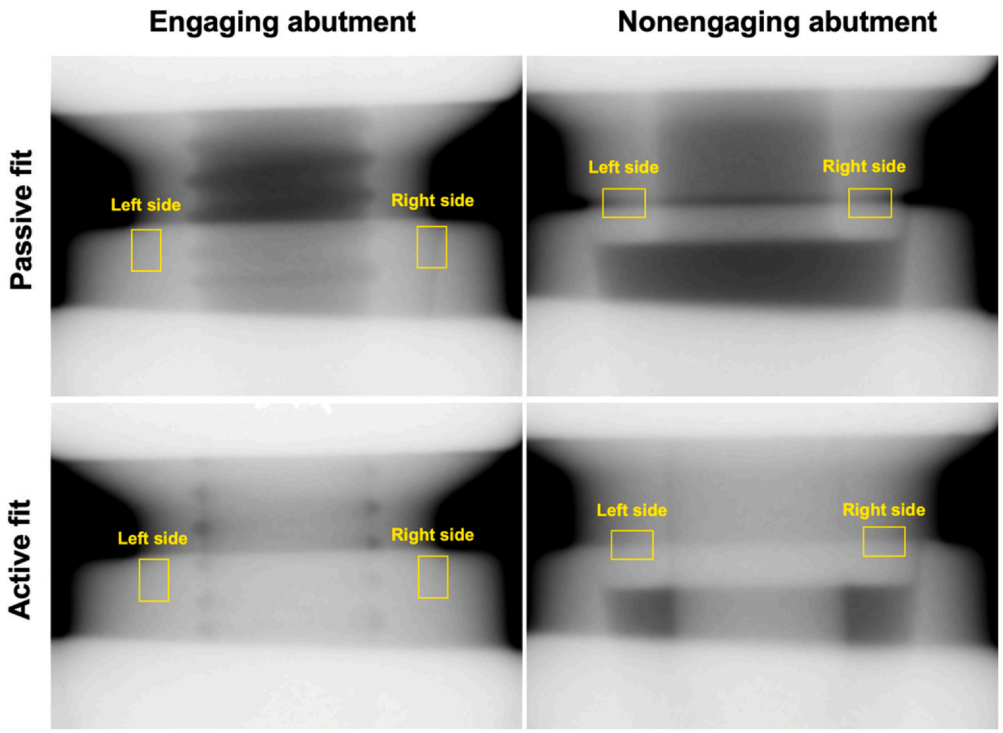

Figure 3. MGV measurements of H70 misfit group on side B implant during passive fit and active fit for engaging (left side) and nonengaging (right side) abutments.

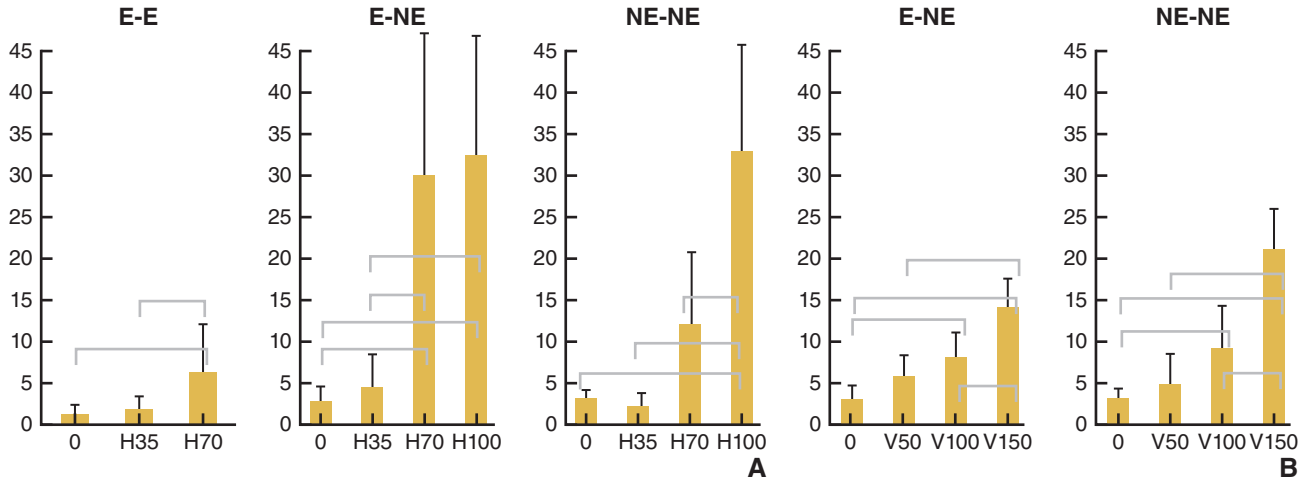

Figure 4. Mean values represent difference in MGV measurements in passive fit and active fit situations for different abutment-type combination groups with different misfit levels. *Brackets* indicate statistically significant differences ($P<.05$) between groups (1-way ANOVA).

observed in either abutment combination group (E-NE and NE-NE) ($P>.05$). In all other measurement comparisons for the vertical misfit, the differences were significant ($P<.05$).

For the horizontal misfit, no statistically significant differences ($P>.05$) between passive and active fit situations were found for all 3 abutment combination groups when H35 was compared with the control group. H100 in the E-NE and NE-NE groups showed significantly different values from all other horizontal misfit levels and from the control groups ($P<.05$). Statistical analysis revealed no significant differences between H70 and H100 in the E-NE group and between H70 and H35 in the NE-NE group ($P>.05$).

Altogether, the differences in MGV measurement between passive fit and active fit were higher for horizontal misfit than vertical misfit, particularly for increased misfit levels.

Table 1. Difference in mean gray values (means and standard deviations) comparing passive to active fit situations (paired samples *t* test)

Connection	Misfit	N	Mean	SD	t	df	*P*
NE - NEPassive to Active	0	10	3.01	1.33	7.17	9	<.001
	H35	10	2.04	1.78	3.63	9	.006
	H70	10	11.95	8.92	4.23	9	.002
	H100	10	32.68	19.61	5.27	9	.001
	V50	10	4.59	3.85	3.76	9	.004
	V100	10	8.92	5.27	5.36	9	<.001
	V150	10	20.85	5.00	13.19	9	<.001
E – NE Passive to Active	0	10	2.71	2.03	4.22	9	.002
	H35	10	4.29	2.95	4.60	9	.001
	H70	10	29.83	11.44	8.25	9	<.001
	H100	10	32.25	37.11	2.75	9	.023
	V50	10	5.48	2.79	6.21	9	<.001
	V100	10	7.58	3.25	7.37	9	<.001
	V150	10	13.80	2.81	11.44	9	<.001
E – E Passive to Active	0	10	1.19	1.18	3.19	9	.011
	H35	10	1.72	2.14	2.54	9	.032
	H70	10	6.12	3.08	6.29	9	<.001

DISCUSSION

As significant differences were found between passive and active fit conditions across different misfit levels for the specimens with different abutment combinations, the null hypothesis that MGV measurements would not show significant differences between the passive and active fit conditions with different misfit levels for the E-NE, E-E, and NE-NE combinations of abutments was rejected.

In previous studies, observers (dentists or radiologists) evaluated misfits, ranging from 1 to 9 in number, on the dental radiographs.[28–32,36] Lin et al[36] reported that up to 30% of the time, radiographic images with no misfit (0 μm microgap) were incorrectly identified as containing a misfit. In another study,[22] 2 radiographic assessments out of 32 were incorrect for the no misfit group, showing that such assessment is subjective. In addition to the influence of different sensors,[31] film holding techniques,[30] X-ray tube angulation,[28,29] and microgap sizes,[28–31,36] misfit assessment was largely dependent on the experience of the operator. This emphasizes a need for objective clinical misfit assessment methods that could facilitate clinical diagnosis.

The present study found no linear correlation between MGV and the degree of misfit. In studies where the microgap was captured radiographically, misfit has been commonly simulated by placing a spacer of the desired height directly at the IAI,[28–32,36] which creates a uniform gap circularly at the IAI. In the present study, misfit was stimulated by moving the implants in a horizontal or vertical direction, thus approximating more closely the clinical scenario where an appearing microgap has different configurations and widths throughout the perimeter.[1] In the case of a misfit, the abutment will usually tighten on one side,[22] resulting in a higher MGV on that side and a lower MGV on the other. In the present study, the average MGV of the left and right aspects of the B side implant was measured, as the mean value could have obscured a misfit. The tightening on one side could also explain the nonlinear relationship between misfit groups. Future studies could compare the lowest MGV instead of the average. For a better understanding of effects caused by misfit in the implant-prosthesis complex, 3-dimensional finite element analysis and X-ray microtomography studies are needed.

Several statistical differences in MGV measurements between passive and active fits were found. For the groups that included the NE type abutment, the difference between passive and active fits generates a higher MGV; subsequently, misfit was easier to detect with this method. The easier detection may be explained by the configuration of the NE abutment, where the projection of its interproximal spaces facilitates the identification of a misfit. However, it seems that statistically significant differences in misfits can only be detected when the simulated horizontal misfit is larger than 35 μm and the vertical one is larger than 50 μm. Accordingly, measuring MGV can be a valid method of detecting larger misfits.

The fabrication errors of frameworks supported by multiple implants have been studied. Uribarri et al[7] measured the marginal discrepancy up to 100 μm in the 1-screw test and between 29 and 42 μm in the final fit test. Al-Meraikhi et al[1] described a 3D marginal discrepancy of up to 135 μm for the 4-unit implant-supported complete arch restoration. Moreover, Tonin et al[26] used a 1-screw test to assess the microgap for 3-unit cantilever FDPs within the range of 32 μm for a framework obtained by computer-aided design and computer-aided manufacturing (CAD-CAM) to 64 μm for a 1-piece cast framework, reporting a 10- to 27-μm microgap after screw tightening. All of the investigated implant prostheses were reported to be clinically acceptable. Notably, for an NE-NE abutment, a horizontal misfit of 35 μm was reported to create a microgap as small as 6.6 μm, and a vertical misfit of 50 μm resulted in a microgap of 11.6 μm in the passive fit.[21] Although

attempts to reach a clinically relevant decision on the acceptable misfit threshold have failed because of the lack of scientific evidence, the heterogeneous study designs and outcomes, and the variety in implant systems and frameworks,[2–4] microgaps of this magnitude have currently been classified as clinically acceptable.

In the present study, higher MGV were observed in horizontal misfits, indicating that this type of misfit caused greater abutment displacements than the vertical type and thus were easier to detect in radiographs. This finding was consistent with the results of the stereometric microgap measurements, where the horizontal misfit values were higher than the vertical ones in the 1-screw test.[21] In addition, since the H35 and H70 misfits in the NE-NE group showed no statistical differences from the control group and each other, the explanation could be the small size of the microgap and its reproduction in the image because of the spatial resolution of the digital sensor. In the previous study, the H35 and H70 misfits in the NE-NE group created microgaps of 6.6 μm and 14.3 μm, respectively, whereas the H100 misfit showed a dramatic rise up to 151 μm.[21] In addition, in the E-NE and E-E groups, the statistically significant rise in the MGV measurements was reported earlier, at the level of H70. Previous studies support the data, indicating that the E component in the framework makes the FDP more sensitive to the misfit.[21,22]

Using the MGV method to detect misfit at the IAI requires the assessment of passive and active fits and subsequently 2 radiograph exposures to determine whether a misfit is present or not. Radiation safety recommendations may contraindicate this method.

Limitations of the study included that because of the different design features of engaging and nonengaging abutments, the same standardized ROI could not be used in both simulated scenarios, and a direct comparison of engaging and nonengaging abutment fits was not possible. However, identifying identical ROI for engaging and nonengaging abutments is necessary in order to obtain directly comparable results. Other limitations included that only 1 type of implant system was analyzed and, as the connection type has been reported to influence the misfit at the IAI,[15,17,27] further studies that include other types of connections and implant systems should be performed before the findings from the present study can be adopted for other systems. As third-party implant prosthetic components can be used with different implant systems, this could further limit the application of the study results to the particular implant system.

The present study was performed in a controlled in vitro setting with the radiograph tube angulation in perfect parallel, essential for diagnostic accuracy.[28,29,36] The clinical situation differs as parallelism could be diminished, and, since implants are submerged in bone, a misfit in bone-level type implants could be difficult to detect.

In this in vitro study, the MGVs of 256 different gray scales were measured. The technology used could be refined by using another software program and different X-ray unit settings (kV, exposure time, and sensor quality). Namely, a higher resolution could produce more distinct differences in radiopaque and radiolucent areas to facilitate MGV calculations. A more obvious distinction between radiopaque and radiolucent areas would reduce the number of exposures from 2 (active and passive) to 1, which is preferable from a radiation perspective. An interesting future application would be to implement this method with artificial intelligence, where an X-ray program could have a built-in function for detecting misfit. The artificial intelligence software available today can detect the implant type.[37,39,40] If it were coupled with a refined MGV analysis adapted to the design of the actual implant, it could indicate whether a misfit is present.

CONCLUSIONS

Based on the findings of the present in vitro study, the following conclusions were drawn:

1. Measuring the mean gray value difference between passive and active fit could be a promising alternative for the detection of microgaps in the implant-abutment connection that result from deviations of 70 to 150 μm.
2. Evaluating the radiographic images with an image processing program revealed some disadvantages: the mean gray value is not yet an adequate measurement for detecting small misfits (< 50 μm) and comparing the microgaps of E and NE abutments because of the different abutment configuration and, thus, the chosen ROI.
3. As 2 radiographic images are not practical in daily practice, checking for misfit should be done with the restoration placed in passive fit.
4. To develop objective misfit assessment methods that could facilitate clinical diagnosis, further investigations are needed regarding the proper selection of regions of interest, X-ray unit settings, clinical protocols with different types of implant-abutment connections, and the application of artificial intelligence tools.

REFERENCES

1. AL-Meraikhi H, Yilmaz B, McGlumphy E, Brantley W, Johnston WM. In vitro fit of CAD-CAM complete arch screw-retained titanium and zirconia implant prostheses fabricated on 4 implants. *J Prosthet Dent*. 2018;119:409–416.

2. Pan Y, Tsoi JKH, Lam WYH, Pow EHN. Implant framework misfit: A systematic review on assessment methods and clinical complications. *Clin Implant Dent Relat Res*. 2021;23:244–258.
3. Katsoulis J, Takeichi T, Sol Gaviria A, Peter L, Katsoulis K. Misfit of implant prostheses and its impact on clinical outcomes. Definition, assessment and a systematic review of the literature. *Eur J Oral Implantol*. 2017;10(Suppl 1):121–138.
4. Abdelrehim A, Etajuri EA, Sulaiman E, Sofian H, Salleh NM. Magnitude of misfit threshold in implant-supported restorations: A systematic review. *J Prosthet Dent* 2022.
5. Abduo J, Lyons K. Effect of vertical misfit on strain within screw-retained implant titanium and zirconia frameworks. *J Prosthodont Res*. 2012;56:102–109.
6. Jimbo R, Halldin A, Janda M, Wennerberg A, Vandeweghe S. Vertical fracture and marginal bone loss of internal-connection implants: A finite element analysis. *Int J Oral Maxillofac Implants*. 2013;28:e171–e176.
7. Uribarri A, Bilbao-Uriarte E, Segurola A, Ugarte D, Verdugo F. Marginal and internal fit of CAD/CAM frameworks in multiple implant-supported restorations: Scanning and milling error analysis. *Clin Implant Dent Relat Res*. 2019;21:1062–1072.
8. Löfgren N, Larsson C, Mattheos N, Janda M. Influence of misfit on the occurrence of veneering porcelain fractures (chipping) in implant-supported metal-ceramic fixed dental prostheses: An in vitro pilot trial. *Clin Oral Impl Res*. 2017;28:1381–1387.
9. Clelland NL, Papazoglou E, Carr AB, Gilat A. Comparison of strains transferred to a bone simulant among implant overdenture bars with various levels of misfit. *J Prosthodont*. 1995;4:243–250.
10. Liu Y. Influences of microgap and micromotion of implant–abutment interface on marginal bone loss around implant neck. *Arch Oral Biol*. 2017;83:153–160.
11. al-Turki LEE, Chai J, Lautenschlager EP, Hutten MC. Changes in prosthetic screw stability because of misfit of implant-supported prostheses. *Int J Prosthodont*. 2002;15:38–42.
12. Jokstad A, Shokati B. New 3D technologies applied to assess the long-term clinical effects of misfit of the full jaw fixed prosthesis on dental implants. *Clin Oral Implants Res*. 2015;26:1129–1134.
13. Janda M, Larsson C, Mattheos N. Influence of misfit on the occurrence of porcelain veneer fractures in implant-supported metal-ceramic fixed dental prostheses. Part 2: A three-dimensional finite element analysis. *Int J Prosthodont*. 2021;34:458–462.
14. Tallarico M, Canullo L, Caneva M, Özcan M. Microbial colonization at the implant-abutment interface and its possible influence on periimplantitis: A systematic review and meta-analysis. *J Prosthodont Res*. 2017;61:233–241.
15. Tsuruta K, Ayukawa Y, Matsuzaki T, Kihara M, Koyano K. The influence of implant–abutment connection on the screw loosening and microleakage. *Int J Implant Dent*. 2018;4:11.
16. Romanos GE, Delgado-Ruiz R, Sculean A. Concepts for prevention of complications in implant therapy. *Periodontol 2000*. 2019;81:7–17.
17. Lauritano D, Moreo G, Lucchese A, Viganoni C, Limongelli L, Carinci F. The impact of implant–abutment connection on clinical outcomes and microbial colonization: A narrative review. *Materials (Basel)*. 2020;13:1131.
18. Sailer I, Strasding M, Valente NA, Zwahlen M, Liu S, Pjetursson BE. A systematic review of the survival and complication rates of zirconia-ceramic and metal-ceramic multiple-unit fixed dental prostheses. *Clin Oral Implants Res*. 2018;29:184–198.
19. Anusavice KJ, Shen C, Rawls HR. Phillips' science of dental materials. 12th ed. St. Louis: Saunders,; 2013:418–473.
20. Savignano R, Soltanzadeh P, Suprono MS. Computational biomechanical analysis of engaging and nonengaging abutments for implant screw-retained fixed dental prostheses. *J Prosthodont*. 2021;30:604–609.
21. Rutkunas V, Dirse J, Kules D, Simonaitis T. Misfit simulation on implant prostheses with different combinations of engaging and nonengaging titanium bases. Part 1: Stereomicroscopic assessment of the active and passive fit. *J Prosthet Dent*. 2023;129:589–596.
22. Rutkunas V, Dirse J, Kules D, Mischitz I, Larsson C, Janda M. Misfit simulation on implant prostheses with different combinations of engaging and nonengaging titanium bases. Part 2: Screw resistance test. *J Prosthet Dent* 2022.
23. Dogus SM, Kurtz KS, Watanabe I, Griggs JA. Effect of engaging abutment position in implant-borne, screw-retained three-unit fixed cantilevered prostheses. *J Prosthodont*. 2011;20:348–354.
24. Kwan JC, Kwan N. The effects of a vertical compressive cyclic load on abutment screws and the stability of the prosthesis in nonengaging and partially engaging abutments in a screw-retained splinted fixed dental prosthesis. *Int J Oral Maxillofac Implants*. 2022;37:571–578.
25. Epprecht A, Zeltner M, Benic G, Özcan M. A strain gauge analysis comparing 4-unit veneered zirconium dioxide implant-borne fixed dental prosthesis on engaging and non-engaging abutments before and after torque application. *Clin Exp Dent Res*. 2018;4:13–18.
26. Tonin BSH, Peixoto RF, Fu J, Freitas BN de, Mattos M da GC de, Macedo AP. Evaluation of misfit and stress distribution in implant-retained prosthesis obtained by different methods. *Braz Dent J*. 2021;32:67–76.
27. Vélez J, Peláez J, López-Suárez C, Agustín-Panadero R, Tobar C, Suárez MJ. Influence of implant connection, abutment design and screw insertion torque on implant-abutment misfit. *J Clin Med*. 2020;9:2365.
28. Sharkey S, Kelly A, Houston F, O'Sullivan M, Quinn F, O'Connell B. A radiographic analysis of implant component misfit. *Int J Oral Maxillofac Implants*. 2011;26:807–815.
29. Papavassiliou H, Kourtis S, Katerelou J, Chronopoulos V. Radiographical evaluation of the gap at the implant-abutment interface. *J Esthet Restor Dent*. 2010;22:235–250.
30. Darós P, Carneiro VC, Siqueira AP, de-Azevedo-Vaz SL. Diagnostic accuracy of 4 intraoral radiographic techniques for misfit detection at the implant abutment joint. *J Prosthet Dent*. 2018;120:57–64.
31. Siqueira AP, Pacheco De Oliveira Mota V, de-Azevedo-Vaz SL. Influence of radiographic acquisition methods and visualization software programs on the detection of misfits at the implant-abutment interface: An ex vivo study. *J Prosthet Dent*. 2022;127:107.e1–107.e7.
32. de-Azevedo-Vaz SL, Araujo-Siqueira C, Carneiro VC, Oliveira ML, Azeredo RA. Misfit detection in implant-supported prostheses of different compositions by periapical radiography and cone beam computed tomography: An in vitro study. *J Prosthet Dent*. 2021;126:205–213.
33. Jörn D, Kohorst P, Besdo S, Borchers L, Stiesch M. Three-dimensional nonlinear finite element analysis and microcomputed tomography evaluation of microgap formation in a dental implant under oblique loading. *Int J Oral Maxillofac Implants*. 2016;31:e32–e42.
34. Kan JY, Rungcharassaeng K, Bohsali K, Goodacre CJ, Lang BR. Clinical methods for evaluating implant framework fit. *J Prosthet Dent*. 1999;81:7–13.
35. Abduo J, Bennani V, Waddell N, Lyons K, Swain M. Assessing the fit of implant fixed prostheses: A critical review. *Int J Oral Maxillofac Implants*. 2010;25:506–515.
36. Lin KC, Wadhwani CPK, Cheng J, Sharma A, Finzen F. Assessing fit at the implant-abutment junction with a radiographic device that does not require access to the implant body. *J Prosthet Dent*. 2014;112:817–823.
37. Park W, Schwendicke F, Krois J, Huh JK, Lee JH. Identification of dental implant systems using a large-scale multicenter data set. *J Dent Res*. 2023;102:727–733.
38. Lee JH, Kim YT, Lee JB, Jeong SN. A performance comparison between automated deep learning and dental professionals in classification of dental implant systems from dental imaging: A multi-center study. *Diagnostics (Basel)*. 2020;10:910.
39. da Mata Santos RP, Vieira Oliveira Prado HE, Soares Aranha Neto I, et al. Automated identification of dental implants using artificial intelligence. *Int J Oral Maxillofac Implants*. 2021;36:918–923.
40. Lee DW, Kim SY, Jeong SN, Lee JH. Artificial intelligence in fractured dental implant detection and classification: Evaluation using dataset from 2 dental hospitals. *Diagnostics (Basel)*. 2021;11:233.

Corresponding author:
Prof Martin Janda
Department of Prosthodontics
Faculty of Odontology
Malmö University
Carl Gustafs väg 34
Malmö SE- 214 21
SWEDEN
Email: martin.janda@mau.se

Acknowledgments
The authors thank Per-Erik Isberg from Lund University (Lund, Sweden) for assistance with statistical analysis.

CRediT authorship contribution statement
Vygandas Rutkunas: Conceptualization, Methodology, Validation, Formal analysis, Resources, Writing - review and editing, Visualization, Supervision, Project administration. **Daniel Kules:** Investigation, Data management, Statistical analysis, Writing - original draft, Visualization. **Ingrida Mischitz:** Data management, Writing - original draft. **Sandra Huber**: Data management, Writing - original draft. **Marta Revilla-León**: Data management, Writing - original draft. **Christel Larsson:** Data management, Statistical analysis, Writing - original draft. **Martin Janda:** Data management, Statistical analysis, Writing - original draft, Visualization, Animations.

Copyright © 2024 The Authors. Published by Elsevier Inc. on behalf of the Editorial Council of *The Journal of Prosthetic Dentistry*. This is an open access article under the CC BY license (http://creativecommons.org/licenses/by/4.0/).

https://doi.org/10.1016/j.prosdent.2024.01.014